orbitals. There are numerous Sc-Sc interactions in Sc_3C_4 with about the same distances as observed in elemental scandium (hcp;[21] each Sc atom has six neighbors at an average distance of 328 pm; the ionic radius of Sc^{3+} is only about 100 pm though!). Since there are only about 4 "excess" electrons per 30 scandium atoms, they certainly could not fill all Sc-Sc bonding states. This rationalization is in agreement with the metallic conductivity and the Pauli paramagnetism of the compound.

Another (additional) possibility to account for the excess electrons concerns the bonding of the scandium atoms to the C(5) atoms. So far we have assumed that the C(5) atoms form two double bonds with their two C(4) neighbors within the C_3 units. This leaves no possibility whatsoever for the C(5) atoms to form bonds to the scandium atoms. The C(5) atoms have two Sc neighbors at 250 pm and two at 267 pm. Even though these distances are considerably greater than the shortest Sc-C distances of 217 pm, one cannot exclude the possibility for weak Sc-C(5) bonding. This can only be achieved if the C(5)-C(4) bonds have a bond order of less than 2. Even small deviations from the full double bonds create many low-lying additional states in the cell (The Lewis formula for propadiene has 16 valence electrons; for propane it has 20.) The C(5)-C(4) bond length of 134.2 pm is indeed slightly greater than the bond lengths of 131.1 and 133.5 pm observed in gaseous propadiene by electron diffraction[22] and by IR spectroscopy,[23] respectively. It is also greater than the average bond length of 130.3 pm observed in six organometallic allenylidene complexes by Berke et al.[24] Thus, in summary the valence electron count agrees rather well with the observed bond lengths.

Acknowledgment. We thank Dr. M. H. Möller and Miss U. Rodewald for the competent collection of single-crystal diffractometer data, K. Wagner for the work on the scanning electron microscope, Dipl.-Phys. Th. Vomhof for the magnetic characterization, and Dipl.-Phys. U. Wortmann for the electrical conductivity measurements. Dr. R. Schwarz (Degussa AG) and Dr. G. Höfer (Heraeus Quarzschmelze) are thanked for generous gifts of palladium metal and silica tubes. This work was supported by the Deutsche Forschungsgemeinschaft and the Fonds der Chemischen Industrie.

Supplementary Material Available: Listings of the crystallographic data and the anisotropic thermal parameters for the scandium atoms of Sc_3C_4 (2 pages); a table of structure factors (3 pages). Ordering information is given on any current masthead page.

(21) Donohue, J. *The Structures of the Elements*; Wiley: New York, 1974.
(22) Almenningen, A.; Bastiansen, O.; Traetteberg, M. *Acta Chem. Scand.* **1959**, *13*, 1699.
(23) Lord, R. C.; Venkateswarlu, Putcha. *J. Chem. Phys.* **1952**, *20*, 1237.
(24) Berke, H.; Härter, P.; Huttner, G.; Zsolnai, L. *Z. Naturforsch., B* **1981**, *36*, 929. Berke, H.; Huttner, G.; von Seyerl, J. *Z. Naturforsch., B* **1981**, *36*, 1277. Berke, H.; Härter, P.; Huttner, G.; von Seyerl, J. *J. Organomet. Chem.* **1981**, *219*, 317. Berke, H.; Härter, P.; Huttner, G.; Zsolnai, L. *Ber. Dtsch. Chem. Ges.* **1982**, *115*, 695. Berke, H.; Härter, P.; Huttner, G.; Zsolnai, L. *Ber. Dtsch. Chem. Ges.* **1984**, *117*, 3423. Berke, H.; Grössmann, U.; Huttner, G.; Zsolnai, L. *Ber. Dtsch. Chem. Ges.* **1984**, *117*, 3432.

Contribution from the Department of Chemistry, Iowa State University, Ames, Iowa 50011

Zirconium Chloride Cluster Phases Centered by Transition Metals Mn-Ni. Examples of the Nb_6F_{15} Structure

Jie Zhang and John D. Corbett*

Received June 25, 1990

Reactions of Zr, $ZrCl_4$, chlorides of Mn-Ni (Z), and LiCl where appropriate in sealed Ta tubing at 750-900 °C yield the dark purple $Li_2Zr_6Cl_{15}Mn$, $LiZr_6Cl_{15}Fe$, $Zr_6Cl_{15}Co$, and $Zr_6Cl_{15}Ni$, all with the basic Nb_6F_{15} structural framework. The structures of all four have been refined by single-crystal X-ray means in the cubic space group $Im\bar{3}m$, $Z = 2$. The a dimensions (Å) and R and R_w (%) are, respectively, as follows: Mn, 10.3459 (4), 2.4, 3.4; Fe, 10.2645 (4), 3.3, 4.2; Co, 10.186 (4), 2.4, 2.0; Ni, 10.1907 (4), 2.1, 3.1. Transition-metal-centered clusters in this structure type are interconnected at all vertices by linear chlorine bridges into three-dimensional ReO_3-like networks $[Zr_6(Z)Cl^i_{12}]Cl^{a-a}_{6/2}$, and two such networks interpenetrate but are unlinked. The relative sizes of the clusters and bridging halogens are critical for this disposition. The lithium atoms in $Li_2Zr_6Cl_{12}Mn$ were refined in an internetwork, six-coordinate site of D_{2h} symmetry, consistent with the solid-state NMR spectrum observed for ^7Li. The expansions of the networks about $Zr-Cl^{a-a}$ necessary to accommodate the lithium ions correspond to volume increments of 12-13 Å^3 for each ion. The effective sizes of the metal interstitials Z increase slightly from Mn to Ni.

Introduction

Among the many centered zirconium chloride cluster compounds,[1] those with the Zr_6Cl_{15} stoichiometry have the greatest structural versatility. These all share a common cluster connectivity, $[Zr_6Cl^i_{12}]Cl^{a-a}_{6/2}$, in which Cl^i is solely edge-bridging within a single cluster while Cl^{a-a} atoms bridge between cluster vertices to generate three-dimensional networks. Four distinctly different architectures are found within this category in terms of both local geometries at the shared Cl^{a-a} and the long-range connectivities of the cluster frameworks.[2-4] Earlier work has provided numerous Zr_6Cl_{15} compositions centered by second-period elements that are distributed among the structure types Ta_6Cl_{15},[5] $KZr_6Cl_{15}C$[3] or $CsNb_6Cl_{15}$,[6] $K_2Zr_6Cl_{15}B$, and $K_3Zr_6Cl_{15}Be$.[4] The first three contain unrelated frameworks, while $K_3Zr_6Cl_{15}Be$ contains a modification of that in $K_2Zr_6Cl_{15}B$. With the aid of these structure types, the relationships between structure type and the size and number of the countercations that must be accommodated in the cluster framework have been well delineated.[4]

Recent successes in incorporating transition metals into the Zr_6Cl_{12} cluster cores have provided more unique cluster compounds.[7] Because of the significant expansion of the clusters that is associated with the change of interstitial from a second-period element to a transition metal, many of these new phases exhibit novel structural features. Differences in the structural behaviors of these two groups of centered clusters are especially obvious in the Zr_6Cl_{15} systems. For instance, with the same stoichiometry but different interstitial elements, $Zr_6Cl_{15}N$[2] adopts the Ta_6Cl_{15} structure whereas $Zr_6Cl_{15}Co$ is based on the novel Nb_6F_{15}

(1) Ziebarth, R. P.; Corbett, J. D. *Acc. Chem. Res.* **1989**, *22*, 256.
(2) Ziebarth, R. P.; Corbett, J. D. *J. Less-Common Met.* **1988**, *137*, 21.
(3) Ziebarth, R. P.; Corbett, J. D. *J. Am. Chem. Soc.* **1987**, *109*, 4844.
(4) Ziebarth, R. P.; Corbett, J. D. *J. Am. Chem. Soc.* **1988**, *110*, 1132.
(5) Bauer, D.; von Schnering, H.-G. *Z. Anorg. Allg. Chem.* **1968**, *361*, 259.
(6) Imoto, H.; Simon, A. Unpublished research.
(7) Rogel, F.; Zhang, J.; Payne, M. W.; Corbett, J. D. *Adv. Chem. Ser.* **1990**, *226*, 369.

0020-1669/91/1330-0431$02.50/0

Table I. Crystal and Refinement Data for $Li_xZr_6Cl_{15}Z$ (x = 2, 1, 0; Z = Mn, Fe, Co, Ni)

formula	$Li_2Zr_6Cl_{15}Mn$	$LiZr_6Cl_{15}Fe$	$Zr_6Cl_{15}Co$	$Zr_6Cl_{15}Ni$
space group, Z	$Im\bar{3}m$ (No. 229), 2	$Im\bar{3}m$ (No. 229), 2	$Im\bar{3}m$ (No. 229), 2	$Im\bar{3}m$ (No. 229), 2
a, Å[a]	10.3459 (4)	10.2645 (4)	10.186 (4)	10.1907 (4)
V, Å^3	1107.4 (1)	1081.6 (1)	1056.9 (1)	1058.3 (1)
abs coeff μ, cm^{-1} (Mo Kα)	50.0	52.5	54.7	56.5
range of transm coeff	0.86–1.00	0.76–1.00	0.62–1.00	0.74–1.00
R,[b] %	2.4	3.3	2.4	2.1
R_w,[b] %	3.4	4.2	2.0	3.1

[a] Guinier powder diffraction results (data from 30, 33, 30 and 27 observations, respectively). [b] $R = \sum||F_o| - |F_c||/\sum|F_o|$; $R_w = [\sum w(|F_o| - |F_c|)^2/\sum w(F_o)^2]^{1/2}$; $w = \sigma_F^{-2}$.

structure.[8] Similarly, $KZr_6Cl_{15}C$ has a modified $CsNb_6Cl_{15}$ structure in which a different cation position is occupied on the basis of cation size, whereas its transition-metal analogue $KZr_6Cl_{15}Fe$ occurs as a superstructure hybrid of the $CsNb_6Cl_{15}$ and $KZr_6Cl_{15}C$ types.[9] The structural differences thus afforded by smaller main-group vs larger transition-metal interstitials allow some clear correlations between the structure type and cluster size to be established.

The present article describes the new cluster compounds centered by transition metals that form with the fourth, Nb_6F_{15}-type framework. Furthermore, the versatility of the series when small cations are included within the lattice in $Li_xZr_6Cl_{15}Z$ phases allows the first direct comparisons to be made for the series of transition-metal interstitials (Z) Mn, Fe, Co, and Ni in a single structural framework. The derivatized Nb_6Fe_{15} examples found are particularly significant, as this novel arrangement of interpenetrating three-dimensional $Nb_6F_{12}F_{6/2}$ networks has remained a structural singularity for over two decades. The present results emphasize how a relatively large metal cluster or a small halide are necessary in order to form this unusual arrangement. The analogous $Th_6Br_{15}Fe$ has also been reported to meet these conditions.[10] On the other hand, this composition is not realized in the analogous zirconium iodide clusters centered by either 3d metals[11] or Si, Ge, P, etc.[12]

Experimental Section

Materials. The quality of the reactor grade zirconium metal, the preparations of $ZrCl_4$ and powdered zirconium, the reaction techniques utilizing welded tantalum containers, and the Guinier powder diffraction and calculation methods have all been described before.[3] All reactants and products were handled only in a glovebox. The LiCl employed was a commercial reagent (Fisher) that had been dried and then sublimed under high vacuum. Metal chlorides that provided the centered transition metals (Z) were prepared by dehydration either in refluxing $SOCl_2$ of $MnCl_2 \cdot 4H_2O$ (Baker analyzed reagent) or $CoCl_2 \cdot 6H_2O$ (Baker and Adamson, reagent grade) or on slow heating in high vacuum of $FeCl_3$ (ROC/RIC, 99%) or $NiCl_2 \cdot 6H_2O$ (Mallinckrodt, analytical reagent). The resulting chlorides were then sublimed under static vacuum in sealed silica tubing (except for $NiCl_2$). Iron powder (Baker, analyzed reagent) was also used in several reactions without giving any difference in product or yield.

Synthetic Observations. The three 18-electron cluster compounds $Li_2Zr_6Cl_{15}Mn$, $LiZr_6Cl_{15}Fe$, and $Zr_6Cl_{15}Co$ can be produced regularly in high yields (>95%) by reactions of $ZrCl_4$, Zr, ZCl_2, and when appropriate, LiCl in stoichiometric proportions at 800–850 °C. On the other hand, only trace quantities of other (probably carbide) cluster materials were obtained on omission of just the ZCl_2 component. However, to facilitate the crystal growth, temperature gradient reactions (950–800 °C, 24 days for $Li_2Zr_6Cl_{15}Mn$; 910–890 °C, 25 days for $LiZr_6Cl_{15}Fe$) were required. The incorporation of lithium in these two phases is supported by the optimal cluster electron count, the observed lattice expansion (below), and the fact that the known ternary 6–14 phases $Zr_6Cl_{14}Mn$ (17 e/cluster) or $Zr_6Cl_{14}Fe$ (18 e/cluster)[9] were formed instead whenever Li was omitted from the reaction system, even if the Zr:Cl ratio was kept at 6:15. In addition, single-crystal X-ray analyses and ^{7}Li solid-state NMR provided further information of the stoichiometry of the manganese phase (below). Reactions with stoichiometries aimed at $Li_xZr_6Cl_{15}Fe$ with x between 0.5 and 1.5 all yielded the new cluster phase with essentially the same lattice constants (plus other products), indicating that a fixed composition with $x \simeq 1$ is controlled by the cluster electron count and not by the proportions loaded. Traces of $ZrFe_2$ could be magnetically separated from some of the iron preparations in amounts sufficient to allow its identification by powder pattern means. Attempts to make a $Li_3Zr_6Cl_{15}Cr$ analogue or any other chromium-containing cluster were unsuccessful. Large crystals of $Zr_6Cl_{15}Co$ were also obtained as the major product from a reaction with the stoichiometry of $KBaZr_6Cl_{18}Co$ (750 °C, 15 days). No 6–18 phase of known structure was identified. An unknown phase (>20 lines, $d_{max} \sim 10.15$ Å) was also obtained in about 40% yield, and since KCl and $BaCl_2$ were both absent from the powder pattern, the unidentified material appears to be a cluster phase rich in K and Ba. This phase or other species evidently serve as a mineralizer for the crystallization of $Zr_6Cl_{15}Co$.

In contrast, $Zr_6Cl_{15}Ni$ was only obtained following reactions designed to obtain the hypothetical 18-electron compounds $M_2Zr_6Cl_{18}Ni$ (M = K, Cs; 850 °C, 25 days and 750–650 °C, 7 days). The yields of nicely formed crystals were high (90% and 80%, respectively) with M_2ZrCl_6 (K_2PtCl_6 type) as the side product. Yet, efforts to produce $Zr_6Cl_{15}Ni$ from a neat reaction with the correct stoichiometry failed to provide the expected result. Altering the proportions of the starting materials, the addition of M^ICl, or variation of the reaction temperature did not solve the problem. Nonetheless, the X-ray studies (below) indicated that the compound under investigation was different from $Zr_6Cl_{15}Co$. Furthermore, EDX spectra collected for several crystals from the above reactions clearly indicated that the only detectable elements in these crystals were Zr, Cl, and Ni, and a semiquantitative analysis gave a composition of $Zr_{5.7}Cl_{14.8}Ni$, identical with $Zr_6Cl_{15}Ni$ within probable experimental errors. Differences in the reactivity of the $NiCl_2$ may be responsible. The source of nickel in the two successful syntheses was $NiCl_2$ from dehydration of the corresponding hydrate, while succeeding reactions employed sublimed material. The latter had been heated ~600 °C higher, and $ZrCl_4$ would doubtlessly compete effectively for MCl and leave the more crystalline $NiCl_2$ insoluble.

Substitution of NaCl for LiCl in the Mn and Fe reactions led to the formation of an unidentified Mn phase and $Zr_6Cl_{14}Fe$, respectively, results that imply that the Na is too large to fit into an Nb_6F_{15}-type lattice. Planned reactions to generate mixed interstitials as $LiZr_6Cl_{15}Mn_{0.5}Co_{0.5}$ and $LiZr_6Cl_{15}Mn_{0.5}Ni_{0.5}$ produced a mixture of two 6–15 phases in the former case and $Li_2Zr_6Cl_{15}Mn$ and an unknown phase in the latter.

NMR Spectra. The spectra of ^{7}Li were studied for ~40-mg samples of $Li_2Zr_6Cl_{15}Mn$ sealed in 7-mm Pyrex tubing under N_2. A Bruker WM-200 instrument was employed with solid LiCl as the reference. No signal for ^{55}Mn ($I = {}^5/_2$) could be found in the expected region.

Structure Determinations. Single-crystal X-ray structural analyses of the complete series at room temperature were conducted in order to allow the direct comparison of the different transition metals as cluster interstitials. As the general structure type was known, the structure determination processes were routine, but precautions were taken to ensure the correct space group especially with Li incorporation. The refinement of cell parameters from powder data suggested that these phases had the expected cubic symmetry, and the body centering was confirmed on the diffractometers. Axial photos were taken to confirm the lattice type and symmetries. No decay correction was necessary in any case, and the data processing included empirical absorption corrections based on ψ-scans and data averaging in the Laue class $Im\bar{3}m$. Some relevant data are given in Table I.

In all the four cases, the interstitial atoms emerged as large residues of about 20 e/Å^3 on the difference Fourier maps after the Zr and Cl atoms had been refined. Their refined occupancies were within the experimental errors for $LiZr_6Cl_{15}Fe$ (102 (1)%) and $Zr_6Cl_{15}Co$ (98 (1)%). On the other hand, a decrease in the occupancies accompanied by a drop in thermal parameters of over 30% was observed for the other two compounds, and the refinements converged with a 92 (1)% filled Mn

(8) Schäfer, H.; Schnering, H.-G.; Niehues, K.-J.; Nieder-Vahrenholz, H. G. *J. Less-Common Met.* **1965**, *9*, 95.
(9) Zhang, J.; Corbett, J. D. Unpublished research.
(10) Simon, A. *Angew. Chem., Int. Ed. Engl.* **1988**, *27*, 175.
(11) Hughbanks, T.; Rosenthal, G.; Corbett, J. D. *J. Am. Chem. Soc.* **1988**, *110*, 1511.
(12) Rosenthal, G.; Corbett, J. D. *Inorg. Chem.* **1988**, *27*, 53.

Table II. Positional and Isotropic Displacement Parameters for $Li_xZr_6Cl_{15}Z$

	x	y	z	B_{iso}, Å^2
		$Li_2Zr_6Cl_{15}Mn$		
Zr	0.2331 (5)	0	0	0.98 (2)
Cl1	0	0.2480 (2)	y	1.46 (3)
Cl2	0	$^1/_2$	$^1/_2$	2.24 (6)
Mn[a]	0	0	0	0.7844 (4)
Li[b]	$^1/_4$	0	$^1/_2$	3 (1)
		$LiZr_6Cl_{15}Fe$		
Zr	0.2361 (1)	0	0	1.50 (3)
Cl1	0	0.2483 (1)	y	1.29 (5)
Cl2	0	$^1/_2$	$^1/_2$	1.8 (1)
Fe	0	0	0	0.79 (9)
		$Zr_6Cl_{15}Co$		
Zr	0.24094 (4)	0	0	0.82 (2)
Cl1	0	0.24883 (6)	y	1.26 (2)
Cl2	0	$^1/_2$	$^1/_2$	1.66 (4)
Co	0	0	0	0.6076 (4)
		$Zr_6Cl_{15}Ni$		
Zr	0.2413 (1)	0	0	0.70 (2)
Cl1	0	0.2485 (1)	y	1.05 (5)
Cl2	0	$^1/_2$	$^1/_2$	1.5 (1)
Ni[a]	0	0	0	1.14 (6)

[a] Full occupancy. [b] The occupancy of Li was fixed at 33%, corresponding to the formula given.

site and an 87 (1)% Ni occupancy. The associated isotropic thermal parameters of Mn (0.557 Å^2) and Ni (0.552 Å^2) were the smallest in each compound, and they were also smaller than those of Fe (0.79 Å^2) and Co (0.61 Å^2) in the other two compounds. The trends suggest that significant coupling between occupancies and thermal displacement parameters may be involved. Moreover, the validity of the alternate model is questionable as far as the chemical and physical meanings are considered. Since a transition-metal interstitial atom contributes a large portion of the electrons for metal–metal bonding in the cluster, it is very unlikely that ~8–13% of the clusters would be empty and hence have a local cluster electron count far from the optimal value of 18. A mixed interstitial model with a light atom does not seem plausible either. Therefore, the problems were attributed to crystallographic errors, and the models with fully occupied interstitial positions were chosen as the best solutions.

Efforts were also made to locate and refine the Li atoms in the Mn and Fe compounds. The refined Nb_6Fe_{15}-type network contains three potential sites for Li atoms, two six-coordinate positions [8*c* at ($^1/_4$, $^1/_4$, $^1/_4$); 12*d* at ($^1/_4$, 0, $^1/_2$)] and one four-coordinate site [48*k* at (x, x, z) with $x \sim {}^3/_8$, $z \sim {}^1/_8$ and Li–Cl = 2.26 Å]. In the case of $LiZr_6Cl_{15}Fe$, no residue higher than 0.3 e/Å^3 was found on the difference Fourier map, and refinement with Li on any of these sites resulted in unreasonably large thermal ellipsoids, negative multiplicities, or both. In $Li_2Zr_6Cl_{15}Mn$, the highest residue peak, 2.3 e/Å^3, was on the 12*d* position. Subsequent refinement of lithium at this position with a fixed occupancy of $^1/_3$, which corresponds to the formula $Li_2Zr_6Cl_{15}Mn$, gave B_{iso} equal to 3 (1) Å^2. As expected, this atom could not be refined either with anisotropic parameters or with the occupancy as an additional variable. Nevertheless, this result appears to confirm the existence of the lithium in the lattice required by the synthetic results (above), and equally important, it provided symmetry information necessary for interpretation of the ^{7}Li NMR spectrum. No residue peak higher than the background (±1 e/Å^3) was found on the other two possible sites. Even in the case of $LiZr_6Cl_{15}Fe$ it is necessary to have close to one lithium per cluster in order to synthesize the phase (above). Systematic variations of the cell volume from $Zr_6Cl_{15}Co$ to $LiZr_6Cl_{15}Fe$ to $Li_2Zr_6Cl_{15}Mn$ (Table I) are also supportive. The cluster cores contract as the lattices expand so significant volume increments must be attributed to each lithium atom, namely 12–13 Å^3. The consistency of the volume changes also suggests that the Li in $LiZr_6Cl_{15}Fe$ occupies the same position as it does in the Mn analogue.

The positional and isotropic displacement parameters for the four compounds are reported in Table II, and important distances are listed in Table III. Additional information is available as supplementary material.

Results and Discussion

The first compound discovered in this series was $Zr_6Cl_{15}Co$. With the 18-electron rule[11] as the guideline, a reaction aimed at this composition was carried out at 850 °C for 30 days. The powder pattern indicated the single product was a 6–15 phase, as expected, but with the cubic structure of Nb_6F_{15} (plus interstitial atom) that had not been previously observed in zirconium systems. The sizes of potential intercluster sites for cations were estimated on the basis of lattice constants, and several sites with a coordination number of 6 or 4 were found that were probably large enough only to accommodate Li^+ ions. Combination of this observation with the cluster electron count expectations led to a prediction of the existence of $Li_2Zr_6Cl_{15}Mn$ and $LiZr_6Cl_{15}Fe$, and these were confirmed soon after by their successful syntheses. The 19-electron $Zr_6Cl_{15}Ni$ was also achievable, but no sodium, bromide, or chromium members of this series could be obtained. All of these phases are dark purple in thicknesses of <0.2 mm when viewed through a microscope. The contrast between this and the red color characteristic of similar clusters centered by main-group elements[1] suggests the present phases probably have appreciably smaller LUMO–HOMO gaps.

Table III. Cluster Electron Counts and Important Interatomic Distances and Angles in $Li_xZr_6Cl_{15}Z$ Phases Based on the Nb_6F_{15} Structure

		$Li_2Zr_6Cl_{15}Mn$	$LiZr_6Cl_{15}Fe$	$Zr_6Cl_{15}Co$	$Zr_6Cl_{15}Ni$
		No. of Cluster Electrons			
		18	18	18	19
		Distances (Å)			
Zr–Zr	(×12)	3.4107 (8)	3.428 (2)	3.4708 (6)	3.477 (1)
Zr–Cl1	(×12)	2.5708 (1)	2.552 (2)	2.5359 (7)	2.533 (1)
Zr–Cl2[a]	(×6)	2.7612 (6)	2.709 (1)	2.6388 (4)	2.636 (1)
Zr–M	(×6)	2.4117 (6)	2.424 (1)	2.4542 (4)	2.459 (1)
Li–Cl1	(×4)	2.607 (2)	2.584 (1)[b]		
Li–Cl2[a]	(×2)	2.5864 (1)	2.566 (1)[b]		
		Angles (deg)			
Cl1–Zr–Cl1[a]		173.13 (4)	174.37 (6)	176.36 (3)	176.69 (5)

[a] Cl2 = Cl^{a-a}. [b] Calculated assuming Li occupies the same position as it does in $Li_2Zr_6Cl_{15}Mn$. [c] Angle to trans Cl^i at cluster vertices.

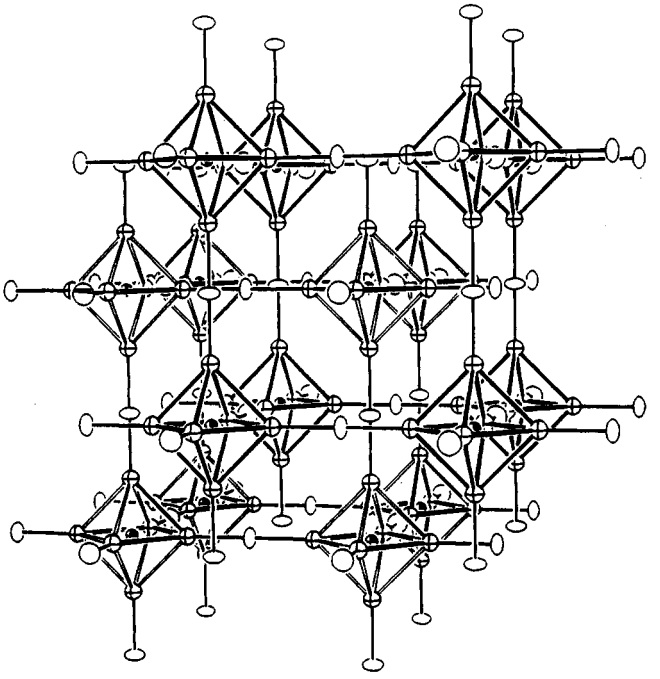

Figure 1. Two identical, interpenetrating $[Zr_6Cl^i_{12}Z]Cl^{a-a}_{6/2}$ networks in the compounds with the Nb_6Fe_{15} structure. They are distinguished by solid and open outlines of the zirconium octahedra. The Cl^i atoms are omitted for clarity.

Structure Description. Each of the four transition-metal-centered cluster phases in the Nb_6F_{15} family contains two identical, independent, and interpenetrating cubic cluster nets of $(Zr_6Cl^i_{12}Z)Cl^{a-a}_{6/2}$ as the main structure framework. This is

depicted in Figure 1 with the omission of Cl^i atoms. This simple yet elegant arrangement demonstrates once again the sophisticated ways in which solid-state materials may be organized. The cluster cores in these phases are perfect octahedra with the high symmetry imposed by the space group. The Zr–Cl^i (Zr–Cl1) distances are normal, decreasing slightly (<0.04 Å) as the cluster cores expand. On the other hand, the Zr–Cl^{a-a} distances are more sensitive to the lithium content and the requisite lattice expansion. As more Li is incorporated into the lattice, the Zr–Cl^{a-a} bonds increase by over 0.12 Å. In addition, the thermal ellipsoids of these bridging atoms appear to reflect a preferred thermal motion or displacement normal to the bridge bonds, a characteristic of halogen in linear bridges that are confined by strong Zr–Cl interactions.[3,13]

The two units in Figure 1 are related by body centering, and each can be viewed as an ReO_3 net that has been expanded by substitution of a large cluster for the rhenium atom, thus enabling two such networks to interpenetrate. Compared with the one-dimensional linear cluster chains in $Ba_2Zr_6Cl_{17}B$,[13] the three-dimensional networks in the Nb_6F_{15} structure are less flexible. Consequently, much more restrictive geometric requirements must be met in order to achieve a fit in this lattice. Accordingly, while $Ba_2Zr_6Cl_{17}Z$ phases exhibit both B and Mn members, the Nb_6F_{15} type only exists among zirconium chloride clusters centered by the larger transition metals.

The size of the cluster core relative to the intercluster bridging halogens is the most crucial condition in this circumstance. The cluster cores centered by transition-metal elements are significantly larger than those containing second-period elements. This expansion produces both Zr–Z distances that are closer to those for Zr–Cl^i and Cl^i–Zr–Cl^i angles across the nearly planar square faces of the cuboctahedra that approach 180° (Table III). Conversely, contraction of the cluster cores in a cubic $^3_\infty[(Zr_6Cl_{12}Z)Cl_{6/2}]$ lattice with linear connections at Cl^{a-a} pulls these terminal Cl^{a-a} atoms toward the center of the cluster and the Cl^i atoms, and the space left within the network for a second, like net eventually becomes insufficient. Thus, analogues of Nb_6F_{15} in Zr–Cl systems were discovered only when transition metals were accommodated in the cluster cores. Although known M_6X_{12}-based cluster phases are large in number, only those few with the M–centroid distances that approach the M–X^a distances may exhibit the Nb_6F_{15} structure. Accordingly, this structure does not exist in the corresponding zirconium bromide systems, while at the other extreme, only fluoride is suitable with clusters constructed from the smaller niobium. The fractional coordinates of the cluster metals in Nb_6F_{15}, $Zr_6Cl_{15}Co$, and $Zr_6Cl_{15}Ni$ are equal within the associated experimental error for the fluoride. These values approach 0.25, which would place that metal midway between the interstitial (origin) and X^{a-a}.

The cluster networks in $Zr_6Cl_{15}Co$ and $Zr_6Cl_{15}Ni$ may be considered as two infinite, neutral molecules entangled together and separated by a van der Waals "skin". When the size criteria are fulfilled, the two cluster nets can coexist comfortably, without enough strain to bend or stretch the linear connections or to cause decomposition. The nearest internetwork contacts Cl^i–Cl^i and Cl^i–Cl^{a-a} in $Zr_6Cl_{15}Co$ are both a relatively comfortable 3.618 (1) Å. The shortest intracluster Cl^i–Cl^i and Cl^i–Cl^{a-a} in this phase are quite similar, 3.585 (1) and 3.601 (1) Å, respectively. The cluster frameworks become charged in the Fe and Mn phases, where they are both expanded and bound by the Li^+ ions, and the internetwork Cl–Cl separations increase by 0.07 and 0.04 Å, respectively, in forming $Li_2Zr_6Cl_{15}Mn$. The extra space required by these lithium props, which occupy only a fraction of the interstices, accounts for the relatively large molar volume increments in the early part of the series, 12–13 $Å^3$ per Li^+ vs 1–2 $Å^3$ estimated for Li^+ by Biltz.[14]

The expansion of the cluster cores observed in this series as the interstitial atom becomes heavier is irregular, the increment in d(Zr–Z) being greatest (0.03 Å) between $LiZr_6Cl_{15}Fe$ and $Zr_6Cl_{15}Co$ and least (0.005 Å) between $Zr_6Cl_{15}Co$ and $Zr_6Cl_{15}Ni$. Except for the Mn–Fe step, the change is opposite to the trend in standard metallic radii, which decrease 0.04 and then 0.01 Å for Fe, Co, and Ni.[15] The Zr–Z distances in the four clusters are also 0.22–0.16 Å less than the corresponding sum of single-bond metallic radii, even though the formal Zr–Z bond order is only $^2/_3$ ($a_{1g}^2t_{2g}^6$). This difference is a common observation in many of these cluster systems and is presumably a result of the formal oxidation of the metal units on cluster formation.[16,17]

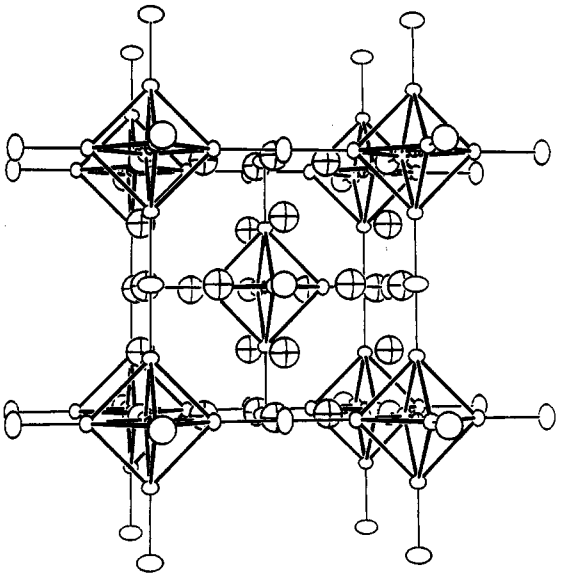

Figure 2. Locations of the four disordered Li^+ ions in the $Li_2Zr_6Cl_{15}Mn$ cell (90% probability thermal ellipsoids). The crossed spheres are Li, and the Cl^i atoms are not shown.

Some of the trends observed in d(Zr–Z) may be the result of matrix effects rather than of a size increase of the centering atoms, as follows. The volume increase noted when lithium is incorporated into the structure may be viewed as a simple stretching of the Zr–Cl^{a-a} bonds, about 0.06 Å/lithium. However, the introduction of strong Li–Cl^{a-a} interactions probably also contributes to a weakening of the Zr–Cl^{a-a} bonds. In either case, a parallel contraction of the cluster core is expected, in accord with the inverse correlation between cluster size (d(Zr–Z)) and Zr–Cl^a distances that has been observed in many cluster systems.[17] A comparison of the rather similar cobalt and nickel examples is more complicated. A 19-electron cluster could be smaller than an 18-electron cluster on the basis of size difference found for the 15-electron $Cs_3Zr_6Cl_{16}C$;[17] however, the extra electron presumably lies in a weakly antibonding orbital that is infrequently occupied. The principal conclusion that can be drawn from this comparison is that the effective radii of the centering atoms are larger in the iodide clusters,[11] probably another result of a matrix effect.

The locations of the lithium atoms in $Li_2Zr_6Cl_{15}Mn$ are depicted in Figure 2; each site is one-third occupied. Among the three possible sites available for four cations per cell, the empty four-coordinate positions (48k) are probably about 0.2 Å too small to accept Li^+. Although the two six-coordinate sites 12d and 8c are similar and sufficient in size and both lie on the zero potential surface that separates the two cluster networks,[18] the former set is favored, probably because they have fewer close zirconium neighbors (4 vs 6). The environment is also consistent with the ^{7}Li NMR spectrum of $Li_2Zr_6Cl_{15}Mn$ (below). Each lithium atom has four cluster units as neighbors (Figure 3). Each of these provides one Cl^i, and each pair of clusters in the same network contributes one Cl^{a-a}. The average Li–Cl distance, 2.60 Å, is in

(13) Zhang, J.; Corbett, J. D. *J. Less-Common Met.* **1989**, *156*, 49.
(14) Biltz, W. *Raumchemie der festen Stoffe*; Leopold Voss Verlag: Leipzig, Germany, 1934; p 238.
(15) Pearson, W. B. *The Crystal Chemistry and Physics of Metals and Alloys*; Wiley-Interscience: New York, 1972; p 151.
(16) Smith, J. D.; Corbett, J. D. *J. Am. Chem. Soc.* **1986**, *108*, 1927.
(17) Ziebarth, R. P.; Corbett, J. D. *J. Am. Chem. Soc.* **1989**, *111*, 3972.
(18) von Schnering, H.-G.; Nesper, R. *Angew. Chem., Int. Ed. Engl.* **1987**, *26*, 1059.

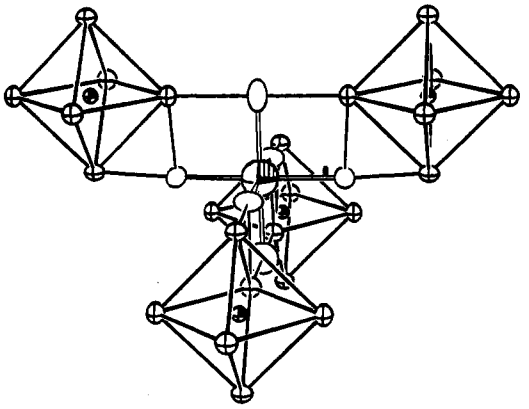

Figure 3. Lithium ion (shaded) and its surrounding cluster units in $Li_2Zr_6Cl_{15}Mn$. Only the neighboring chlorine atoms are shown (open ellipsoids). The site possesses D_{2d} symmetry with the S_4 axis vertical and one of the mirror planes in the plane of the paper (90% probability).

reasonable agreement with the sum of crystal radii, 2.57 Å.[19] Replacing the lithium with a larger cation would require substantial expansion of the lattice via increased Zr–Cl^{a-a} distances. The largest Zr–Cl^{a-a} separation known, 2.76 Å, occurs in $Li_2Zr_6Cl_{15}Mn$, and it is possible that any further stretching of this bond will destabilize the entire lattice. Sodium derivatives of this structure could not be obtained, and $KZr_6Cl_{15}Fe$ has another arrangement. Interestingly, a twisted version of a single ReO_3-like network (PdF_3-like) is found in $Cs_3(ZrCl_5)Zr_6Cl_{15}Mn$.[9]

NMR Studies. Although it is evident that lithium is essential to the syntheses and that this ion also plays important structural and electronic roles in the formation of $Li_2Zr_6Cl_{15}Mn$ and $LiZr_6Cl_{15}Fe$, a study of ^7Li NMR spectra was considered desirable to confirm the results of the single-crystal X-ray analyses, particularly since the cations in these seem to be disordered over one-third or one-sixth of one particular site, respectively. The room-temperature solid-state NMR spectrum of ^7Li in $Li_2Zr_6Cl_{15}Mn$ contains a single triplet centered at −0.4 ppm (vs LiCl) (Figure 4). The peak profile is completely different from that of LiCl, which gives a typical Gaussian singlet, and clearly indicates that the lithium in the sample is not LiCl. The splitting of the signal corresponds to a noncubic symmetry ($Q_c \neq 0$), the symmetric arrangement of the two satellites implies that only one type of site is being seen, and the small chemical shift with respect to solid LiCl suggests that the chemical environments in LiCl and in the sample are similar. The signal was assigned to $Li_2Zr_6Cl_{15}Mn$ since no other lithium-containing phase was observed in the powder pattern.

However, the above observations are not sufficient to derive the exact cation location in the lattice. All of the three possible cation sites in the Nb_6F_{15} structure have noncubic symmetries ($Q_c \neq 0$). The two six-coordinate sites have axial symmetry and hence zero asymmetry parameters ($\eta = 0$), while the distorted tetrahedral site (CN = 4) would have $\eta \neq 0$. Yet, comparisons of the spectrum with the idealized line shapes for a nucleus with $I = {}^3/_2$ only rule out the possibility of $\eta = 1$. Identification of another pair of satellites would be necessary to determine both Q_c and η. Attempts were made without success to locate additional peaks, including the use of increased scan time, an increased amount of sample, and sample cooling. Artificial enhancement of the signal height or use of the spectrum derivative did not help either. It is very likely that the shoulders or steps are lost in the background due to the line broadening. One of the possible solutions to this problem, spinning the sample, was not available because of the necessity of working with a sealed container.

Nevertheless, the study can be concluded by combining the results of NMR studies and the X-ray analysis. The structure solution indicates that lithium occupies a position with D_{2d} point symmetry, and therefore the asymmetry parameter η associated with this should be zero. With this additional information, the

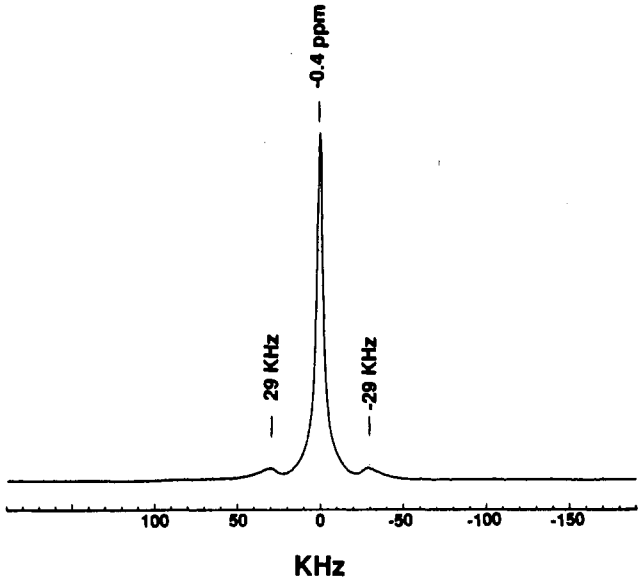

Figure 4. Room-temperature solid-state NMR spectrum of ^7Li in $Li_2Zr_6Cl_{15}Mn$ (static sample; LiCl (s) reference).

quadrupole coupling constant is determined to be 58 kHz. The value is qualitatively consistent with the 0.02-Å axial compression of the coordination polyhedron, especially since the axial Cl^{a-a} atoms are more distant from zirconium and generally appear to be more negative in their interactions with cations in diverse cluster compounds.[1,9,17]

Because the lithium atoms are located on the zero potential surface in the lattice, comparable to the situation with Ag^+ in α-AgI, it is possible that the Li^+ ions in $Li_2Zr_6Cl_{15}Mn$ may have a relatively high mobility under some circumstances. The lack of a significant change in line shape in the NMR spectrum at 173 K suggests that the thermal motions of lithium at both temperatures are comparable. Since AgI becomes a significant solid electrolyte only above 419 K, it is logical that experiments above room temperature will be necessary in order to detect any mobility changes in $Li_2Zr_6Cl_{15}Mn$. A solid-state NMR study of ^7Li in $LiZr_6Cl_{15}Fe$ could not be conducted because of the minor ferromagnetic impurities, probably $ZrFe_2$, that caused the sample to move in response to the field. Traces of magnetic impurities have so far precluded magnetic susceptibility measurements on the four compounds in this group, as well as all other transition-metal-centered cluster phases except for $Zr_6I_{12}Mn$.[11]

The discoveries presented herein again highlight (a) the versatility of interstitial substitutions possible in halide clusters of the early transition metals and (b) the novel compositional and structural variations that may be achieved thereby. Whether the zirconium halide systems will also provide examples of centered platinum metals recently uncovered for rare-earth-metal iodide clusters[20] is not yet known.

Acknowledgment. The NMR studies were ably carried out by V. Rutar of the Departmental Instrumental Services. The first powder samples of $Li_2Zr_6Cl_{15}Mn$ were prepared by T. R. Hughbanks. This research was supported by the National Science Foundation, Solid State Chemistry, via Grants DMR-8318616 and DMR-8902954 and was carried out in facilities of the Ames Laboratory, DOE.

Registry No. Zr, 7440-67-7; $ZrCl_4$, 10026-11-6; $FeCl_2$, 7758-94-3; $MnCl_2$, 7773-01-5; $CoCl_2$, 7646-79-9; $NiCl_2$, 7718-54-9; $Li_2Zr_6Cl_{15}Mn$, 130668-76-7; $LiZr_6Cl_{15}Fe$, 130668-77-8; $Zr_6Cl_{15}Co$, 130668-78-9; $Zr_6Cl_{15}Ni$, 130668-79-0; Ni, 7440-02-0; Co, 7440-48-4; Fe, 7439-89-6; Mn, 7439-96-5.

Supplementary Material Available: Tables of more crystal and refinement data and of anisotropic displacement parameters for $Li_2Zr_6Cl_{15}Mn$, $LiZr_6Cl_{15}Fe$, $Zr_6Cl_{15}Co$, and $Zr_6Cl_{15}Ni$ (2 pages); tables of observed and calculated structure factors for the same compounds (6 pages). Ordering information is given on any current masthead page.

(19) Shannon, R. P. *Acta Crystallogr. Sect. A* **1976**, *A32*, 751.

(20) Payne, M. W.; Corbett, J. D. *Inorg. Chem.* **1990**, *29*, 2246.